Journal of Medicine in Scientific Research

Volume 5 | Issue 3 Article 16

Subject Area:

Role of MRI in evaluation and characterization of neoplastic and nonneoplastic cardiac masses

Ibraheim M. Helmy
General Organization for Teaching Hospitals and Institutes (GOTHI)

Yara M. A. Ziada
General Organization for Teaching Hospitals and Institutes (GOTHI), yaraziada@gmail.com

Recommended Citation

Helmy, Ibraheim M. and A. Ziada, Yara M. (2022) "Role of MRI in evaluation and characterization of neoplastic and nonneoplastic cardiac masses," *Journal of Medicine in Scientific Research*: Vol. 5: Iss. 3, Article 16.
DOI: https://doi.org/10.4103/jmisr.jmisr_26_22

Original Article

Role of MRI in evaluation and characterization of neoplastic and nonneoplastic cardiac masses

Ibraheim M. Helmy, Yara M.A. Ziada

Department of Radio-Diagnosis, General Organization for Teaching Hospitals and Institutes (GOTHI), Cairo and Zagazig, Egypt

Abstract

Background

The overall frequency of cardiac tumors is quite low, with an estimated cumulative prevalence of 0.002–0.3% at autopsy, however, they represent an important group of cardiovascular abnormalities as the early and accurate diagnosis maybe curative and sometimes avoids unnecessary surgery.

Aim and objectives

The aim of this study was to evaluate the efficacy of MRI, in diagnosis, evaluation, and characterization of cardiac neoplasms, as identification and differentiation between the cardiac masses are of extreme importance to develop exquisite better therapeutic planning and positive prognostic results.

Patients and methods

This study is a prospective one that was conducted on 27 patients who were diagnosed to have cardiac masses by echocardiography or other imaging modalities. Contrast-enhanced MRI was done on closed Siemens MR Systems operating at 1.5 T in National Heart Institute in Giza. The study was performed after approval of the Ethical Committee of Scientific Research. Evaluation of cardiac masses was analyzed, regarding the involved chambers, pericardial violation, morphological characters, as well as their pattern of enhancement at contrast-enhanced cardiac MRI studies, aiming at characterization of different cardiac masses on MRI diagnostic bases.

Results

In our study, we diagnosed 85.2% (23/27) of the cases as benign-looking lesions (including both true and pseudotumors), while 14.8% (4/27) as malignant-looking lesions. A statistical significant difference was noted, regarding the differentiation between the benign and the malignant lesions regarding the size, marginal outline, pattern of growth, and pericardial affection, either infiltration or effusion. As regards the pericardial affection, none of the benign lesions showed pericardial infiltration compared with 50% (2/4) of the malignant lesions that showed pericardial infiltration with a statistically significant *P* value of 0.017.

Conclusion

Cardiac magnetic resonance imaging (CMR) has a great role in evaluation of the cardiac masses by its powerful assessment of the anatomical and soft-tissue characterization of the masses, as well as their functional impact, and so it allows the differentiation between neoplastic and nonneoplastic masses, as well as between malignant and benign masses.

Keywords: Cardiac masses, cardiac MRI, thrombus, myxoma

Introduction

The overall frequency of cardiac tumors is quite low, with an estimated cumulative prevalence of 0.002–0.3% at autopsy and 0.15% in echocardiographic series [1], however, they represent an important group of cardiovascular abnormalities as the early and accurate diagnosis maybe curative and sometimes avoids unnecessary surgery [2].

Access this article online

Quick Response Code:

Website: www.jmsr.eg.net

DOI: 10.4103/jmisr.jmisr_26_22

Thrombus is the most common entity followed by metastasis. While myxomas and sarcomas account for

Correspondence to: Dr. Yara M.A. Ziada, MSC, FEBR MD, Elahrar Teaching Hospital, Zigzag, Sharkia. Postal Code: 44514; Tel: 0552362742; Fax: 0552362739; E-mail: yaraziada@gmail .com

Submitted: 09-Mar-2022 **Revised:** 07-May-2022 **Accepted:** 07-May-2022 **Published:** 23-Nov-2022

How to cite this article: Helmy IM, Ziada YM. Role of MRI in evaluation and characterization of neoplastic and nonneoplastic cardiac masses. J Med Sci Res 2022;5:300-8.

most tumors in adults, rhabdomyomas are the most frequent in infants and fibromas are the most common in children [3].

Echocardiography is the primary modality for imaging the intracardiac diseases. However, as image acquisition with MRI has steadily become faster, these modalities have played an increasingly important role in the evaluation of cardiac neoplasms [1].

MRI provides a noninvasive and three-dimensional assessment of the masses involving the cardiac chambers, the pericardium, and the extracardiac structures [4]. The goal of MRI is for assessing cardiac and paracardiac masses, including the confirmation or exclusion of the masses suspected by any other modalities, confirming their location, mobility, and relationship to the surrounding tissues [5].

MRI has become a promising method to yield complementary diagnostic information and to guide cardiac surgeons in the design of an appropriate therapeutic strategy [4].

Patients and Methods

This is a descriptive analytical study aimed to evaluate the role of contrast-enhanced cardiac MRI in characterization of cardiac masses on 27 patients who were diagnosed to have cardiac masses by echocardiography or other imaging modalities. MRI of the selected cases was done on closed (Siemens MR Systems, Munich Germany) operating at 1.5 T in National Heart Institute in Giza. The study was performed after approval of the Ethical Committee of Scientific Research. Patients were consented to participate in this research work.

Adequate personal history review was done for the study-group patients, including the age, complaint, history of present illness, past-history review, including previous myocardial infarctions, primary malignant lesions and previous central line or porto-cath insertion, as well as surgical history review.

Patients were excluded if any contraindication for MRI was present, including claustrophobic patients, patients with significant arrhythmias (such as atrial fibrillation or frequent premature ventricular contractions), patients with bad general condition, or those known to have contraindications for MRI, like an implanted magnetic device, pacemakers (must be adapted first), or mechanical valve prosthesis (absolute contraindication). Patients whose contrast-material safety had not been proved, such as lactating and pregnant females, and those who have acute renal injury, chronic kidney disease, renal failure, and any categories, where glomerular filteration rate less than 30 ml/min or serum creatinine more than 1.5 mg/dl.

Patient preparation, including reassurance, respiratory training, and adaptation of pacemaker if needed.

The study was performed with a 1.5-T MR system (Siemens MR Systems operating). The patients lie on the MRI table in supine position. The ECG electrodes were placed on the sternum and fingers in all cases after cleaning the skin. Then, specific cardiac or torso coils were used for imaging with multielement phased-array coils (16 channels), required for parallel imaging.

Image acquisition

ECG-gated MRI of the heart was performed with leads on chest wall. Multislice transverse spin-echo images were acquired with a slice thickness of 8–10 mm and an interslice gap of 2 mm in adults, and a slice thickness of 5 mm and an interslice gap of 1 mm in children. TA is equal to the AR interval, and TE is 20–30 ms. Coronal, sagittal, or oblique images, depending on the anatomy of the region of interest, were acquired.

Additional gradient-recalled echo- (GRE) dine MRI were acquired in both transverse and coronal planes. The TA is 40–50 ms and the TE is 22 ms. Localizer images were in three orthogonal planes that were taken first. ECG steady-state free precession (balanced fast field echo) cine sequence was used.

FSE sequences (black-blood pool) were taken in axial, sagittal, and coronal views with the following sequence parameters: repetition time in ms (TR)/echo time in ms (TE), 800–1666/28–40; field of view (FOV), 75.5 × 38; section thickness (ST), 3 mm.

T2 STIR sequence was taken in short-axis view with the following parameters: repetition time in ms/echo time in ms, 800–1666/80; section thickness (ST), 8 mm; FOV, 103 × 51.7. GRE sequences (white-blood pool) were taken in vertical long-axis, short-axis (SA), and four-chamber (4CH) views with the following sequence parameters:

Sequence parameters of vertical long-axis: repetition time in ms/echo time in ms, 2.7–2.9/1.34–1.45; flip angle (FA), 60°; section thickness, 8 mm; FOV, 97 × 49.3.

Sequence parameters of 4CH: repetition time in ms/echo time in ms, 2.8–3/1.5–1.7; flip angle, 60°; section thickness, 8 mm; FOV, 87.7 × 44.2.

Dynamic MRI sequence

The contrast used was of a dose 0.3 ml/kg and was injected through the cannula into an upper-limb vein with a flow rate of 3 ml/s.

Imaging in SA and 4CH views in T1-weighted images with long TI was obtained.

Lock-locker sequence

This was used to assess the inversion time (TI), which was important to null the signal intensity of the normal myocardium after contrast-agent administration So, the normal myocardium appeared dark against the abnormally enhanced myocardium. The acquisition was performed in SA view.

Delayed-enhancement cardiac MRI

This was done using contrast-enhanced inversion-recovery sequence after 10–30 min after contrast injection. Imaging of the left ventricle was done from base to apex, and the acquisition was performed in SA and 4CH views. Images were acquired during end-expiration breath hold.

Statistical methods

Data collected throughout history, basic clinical examination, laboratory investigations, and outcome measures were coded, entered, and analyzed using Microsoft Excel software. Data were then imported into Statistical Package for the Social Sciences (SPSS, version 20.0, Chicago, USA) (Statistical Package for the Social Sciences) software for analysis. According to the type of data, qualitative represents as number and percentage, quantitative continues to the group represented by mean ± SD, the following tests were used to test differences for significant difference and association of the qualitative variable by χ^2 test. Differences between quantitative independent groups by *t* test or Mann–Whitney, paired by paired *t*. *P* value was set at less than 0.05 for significant results and less than 0.001 for high significant result.

Data were collected and submitted to statistical analysis. Statistical tests and parameters used in our research work included mean, SD, and χ^2.

Cardiac MRI analysis

Cardiac MRI were analyzed to comment on the cardiac mass characteristics as regards their l`ocation number of the lesions, size, mobility of the lesions, hemodynamic impact of the lesions, marginal outlines of the lesions, signal intensity compared with the normal myocardium on black-blood-pool (FSE) images, white-blood-pool (GRE) images, and early and late contrast-study images, signal pattern homogeneous or heterogeneous of the cardiac masses, presence of pericardial or pleural effusion, presence of pericardial infiltration, and other extracardiac findings.

Two radiologists gave either single diagnosis or differential diagnosis as regards each case. The final diagnosis was compared with the clinical, surgical evaluation of the patients, as well as their therapeutic response to the treatment with or without follow-up by echocardiography.

Results

The diagnoses were collected after commenting on certain items as regards the size, number, location, mobility, hemodynamic impact, marginal outline of the lesions, signal intensity compared with the normal myocardium on black-blood-pool (FSE) images, white-blood-pool (GRE) images, and early and late contrast-study images, signal pattern (homogeneous or heterogeneous) of the cardiac masses, presence of pericardial effusion, presence of pericardial infiltration, and other extracardiac findings.

The studied population included 27 patients, eight (29.6%) females and 19 (70.4%) males. The median age group was 45 years with interquartile range from 34 to 60 years, while the maximum-to-minimum range was from 1 month to 81 years (Table 1).

About 48.2% (13/27) of the studied population had no relevant clinical data, 14.8% (4/27) had ISHD, 7.4% (2/27) had history of primary malignant neoplasm, 11.1% (3/27) had history of central venous line or porta-cath insertion, 11.1% (3/27) had history of both primary malignant neoplasm and central venous line or porta-cath insertion, and 7.4% (2/27) had history of coagulopathy disorders (Tables 2–5).

From the 27 cases, 21 (77.8%) cases show only a single cardiac mass lesion, while six (22.2%) cases show multiple lesions. The median cross-sectional area was 2.2 cm^2 with interquartile range from 1.2 to 7.7 cm^2, while the maximum-to-minimum cross-sectional area was from 0.4 to 28.2 cm^2.

In our study, the most commonly involved cardiac chamber by the cardiac masses was the right atrium by 51.9% (14/27) followed by the right ventricle by 29.6% (8/27). The left atrium was involved by 22.2% (6/27) and the least cardiac-chamber involvement was the left ventricle by 18.5% (5/27). The interatrial septum was affected in 18.5% (5/27) of the cases, the interventricular septum was affected in 22.2% (6/27) of the cases, and the inferior vena cava was affected in 18.5% (5/27) of the cases in our study population, as illustrated in Chart 1.

As regards the characteristics of the cardiac masses in our study, we found that 40.7% (11/27) were mobile lesions, while 59.3% (16/27) were immobile lesions, as described in Chart 2, 92.6% (25/27) showed localized growth pattern, while

Table 1: Characteristics of the study population

Variables	*n* (%)/median (IQR)
Sex	
Male	19 (70.4)
Female	8 (29.6)
Age (years)	45 (34-60); range, 1 month to 81 years

IQR, interquartile range.

Table 2: Relevant clinical data

Variables	*n* (%)
Relevant clinical data	
Nil	13 (48.2)
History of ISHD	4 (14.8)
History of 1ry tumor	2 (7.4)
History of CVC/porta-cath insertion	3 (11.1)
History of 1ry tumor and CVC/porta-cath insertion	3 (11.1)
History of coagulopathy disorder	2 (7.4)

Table 3: Nature of mass

Variables	*n* (%)
Nature of the mass	
True tumor	12 (44.4)
Pseudotumor	13 (48.1)
Undefined	2 (7.4)

In our study, the statistical significant items in the differentiation between the true and the pseudotumors were the marginal outline, the affected cardiac chamber, and the pattern of delayed enhancement as well as the relevant clinical data.

Table 4: Analytic features of the study variables, and corresponding *P* values

Variables	True tumor (*N*=12)	Pseudotumor (*N*=13)	*P*
Age (years)	41.5 (0.9-60)	48 (38-56.5)	0.205¶
Cross-sectional area (cm^2)	5.1 (1.8-17.5)	1.6 (1.1-4.8)	0.051¶
Sex, male/female	8/4	9/4	1.000§
Multiplicity of lesions (single/multiple)	9/3	10/3	1.000§
RA involvement	6 (50.0)	7 (53.8)	0.848¥
LA involvement	4 (36.4)	1 (7.7)	0.142§
RV involvement	7 (58.3)	1 (7.7)	0.011§
LV involvement	2 (16.7)	3 (23.1)	1.000§
IAS involvement	5 (41.7)	0	0.015§
IVS involvement	5 (41.7)	1 (7.7)	0.073§
IVC involvement	2 (16.7)	2 (15.4)	1.000§
Lesion mobility (mobile/immobile)	4/8	6/7	0.688§
Lesion pattern (localized/diffuse infiltrative)	10/2	13/0	0.220§
Lesion outlines (regular/irregular)	7/5	13/0	0.015§
Signal pattern (homogeneous/heterogeneous)	9/3	10/3	1.000§
Signal intensity (black-blood-pool images)			0.372§
Hypointense	4 (33.3)	8 (61.5)	
Isointense	7 (58.3)	4 (30.8)	
Hyperintense	1 (8.3)	1 (7.7)	
Signal intensity (white-blood-pool images)			0.320§
Hypointense	4 (33.3)	8 (61.5)	
Isointense	6 (50.0)	3 (23.1)	
Isointense to hyperintense	2 (16.7)	2 (15.4)	
Pattern of delayed enhancement			<0.001§
Nil	2 (16.7)	12 (92.3)	
Faint	6 (50.0)	0	
Moderate	2 (16.7)	0	
Intense	1 (8.3)	0	
Peripheral	1 (8.3)	1 (7.7)	
Pericardial infiltration	2 (16.7)	0 (0)	0.220§
Pericardial effusion	3 (25.0)	0	0.096§

¶Mann-Whitney test. §Fisher's exact test. ¥Pearson chi-squared test.

7.4% (2/27) showed infiltrative diffuse pattern as described in Chart 3, 81.5% (22/27) showed regular outline, and 18.5% (5/27) showed irregular outline, as illustrated in Chart 4.

About 7.4% (2/27) of the cases showed pericardial infiltration, while 11.1% (3/27) showed pericardial effusion.

In our study, we found that 13 (48.1%) cases were diagnosed as nonneoplastic masses (pseudotumors), 12 (44.4%) cases were diagnosed as true tumors either benign or malignant looking, and two (7.4%) cases were undefined and needed further investigations to recognize the nature of the cardiac masses.

In our study 84.4% (11/13) of the masses diagnosed as pseudotumors were diagnosed as intracardiac thrombus. The others were diagnosed as focal hypertrophied cardiomyopathy and hypertrophied crista terminalis.

According to our study results, the statistical significant items in the differentiation between the true and the pseudotumors were the marginal outline, the affected cardiac chamber, and the pattern of delayed enhancement as well as the relevant clinical data.

We found that all detected pseudotumors showed regular outline compared with 58.3% (7/12) of the true tumors and that attends a statistically significant *P* value 0.015 (significant $P < 0.05$). About 92.3% (12/13) of the cases that were diagnosed as pseudotumors showed no enhancement in the delayed contrast images compared with 16.7% (2/12) of the true tumors with a statistically significant *P* value less than 0.001 as described in Table 4.

In our study, we diagnosed 85.2% (23/27) of the cases as benign-looking lesions (including both true and pseudotumors), while 14.8% (4/27) as described in Table 5.

We found that statistical significant items in the differentiation between the benign and the malignant lesions were including the size, marginal outline, pattern of growth, and pericardial affection, either infiltration or effusion (Figs. 1–3).

Discussion

Cardiac masses have a variety of differential diagnosis ranging from nonneoplastic lesions (pseudotumors) as thrombus to neoplastic lesions, either benign or malignant lesions.

Table 5: Characteristics of true tumors and pseudotumors

Variables	True tumor (*N*=12)	Pseudotumor (*N*=13)	*P*
Associated clinical data			<0.001§
Irrelevant	11 (91.7)	1 (7.7)	
History of ISHD	0	3 (23.1)	
History of 1ry tumor	1 (8.3)	1 (7.7)	
History of CVC/porta-cath insertion	0	3 (23.1)	
History of 1ry tumor and CVC/Porta-cath insertion	0	3 (23.1)	
History of coagulopathy disorders	0	2 (15.3)	
Preliminary impression by MRI			0.039§
Benign-looking	8 (66.7)	13 (100.0)	
Malignant-looking	4 (33.3)	0	
Course by radiologic follow-up			0.006§
Stationary course	4 (100.0)	0	
Organization of thrombus	0	4 (57.1)	
Resolution of thrombus	0	2 (28.6)	
Cardiac CT- and TTE-confirmed diagnosis (crista terminalis)	0	1 (14.3)	

Data are presented as median (interquartile range), ratio, or number (valid %). §Fisher's exact test.

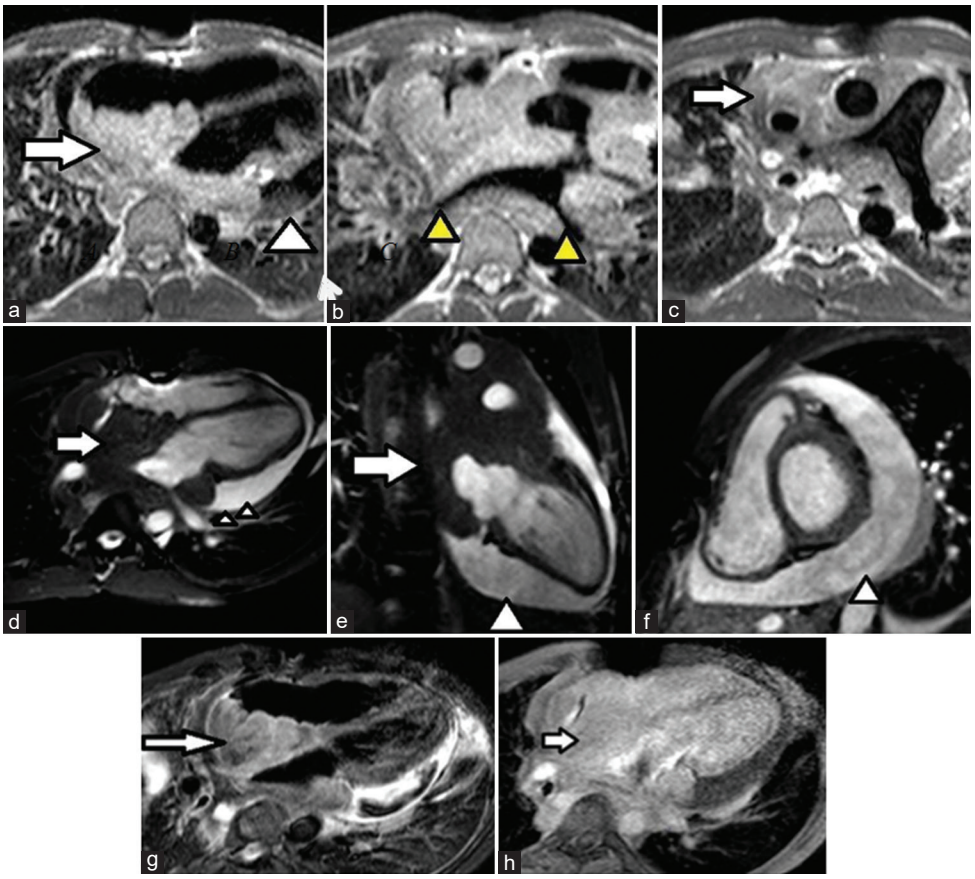

Figure 1: 25 year old male complains of dyspnea &orthopnea for one month duration. His echo reveals dilated thickened walls of both atria with pericardial effusion suspecting restrictive VS constrictive pericarditis. CMR is recommended (a, b, and c). Axial black blood pool T1W images show infiltrative soft tissue lesion (white arrows in a, and c) involving both atrial chamber particularly the right one with squeezing of the SVC and pulmonary veins (yellow arrow heads, in b). It also encases the ascending aorta and pulmonary trunk, and SVC. (arrow in c) This lesion exhibits iso- intense signal in T1WI. Focal LT pulmonary infiltration was noted at (white arrow head in a). White blood pool images (d) four chamber view, (e) vertical long axis and (f) short axis view; show the infiltrative lesion (white arrow) involving the both atria, encasing the aorta & pulmonary trunk. It exhibits iso- intense signal intensity. Also pericardial effusion is detected (arrow heads). (g) STIR four chamber view image shows no signal drop denoting absence of fat. (h) Delayed post contrast image four chamber view shows faint heterogeneous contrast enhancement of the infiltrative mass lesion (arrow). MR features suggestive of lymphomatous infiltration (primary cardiac lymphoma), that was confirmed by pathological evaluation.

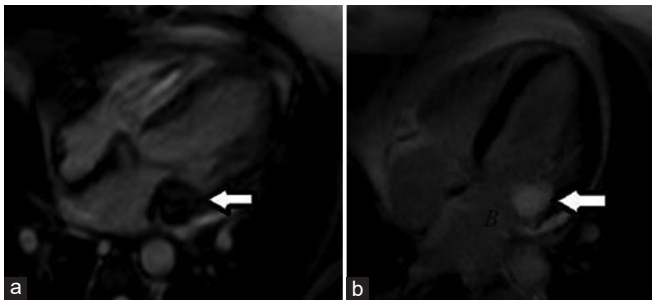

Figure 2: 67 year old female was referred to the MRI unit with left atrial mass as diagnosed by echocardiography. CMR is requested for better characterization of the lesion. (a) White blood pool four chamber view image shows a soft tissue mass lesion arising from the atrial aspect of the posterior mitral leaflet (arrow). (b) Delayed post contrast image shows homogeneous enhancement of the mass lesion (arrow) the mass was confirmed to be myxoma, by histo-pathological evaluation.

Nonneoplastic lesion usually needs medical treatment, while neoplastic lesions usually need surgical intervention. Accurate diagnosis is important to avoid unnecessary surgical intervention.

Cardiac neoplasm is classified into primary and secondary. Primary benign cardiac tumors are more common than primary malignant lesions, while cardiac metastasis is much more common than primary tumors.

In our study, thrombi showed variable signal intensity (SI) in both black-blood-pool and white-blood-pool images, mostly low SI in both black-blood-pool and white-blood-pool images. All cases showed no enhancement in delayed postcontrast images apart from only one case that showed peripheral enhancement consistent with chronic thrombus.

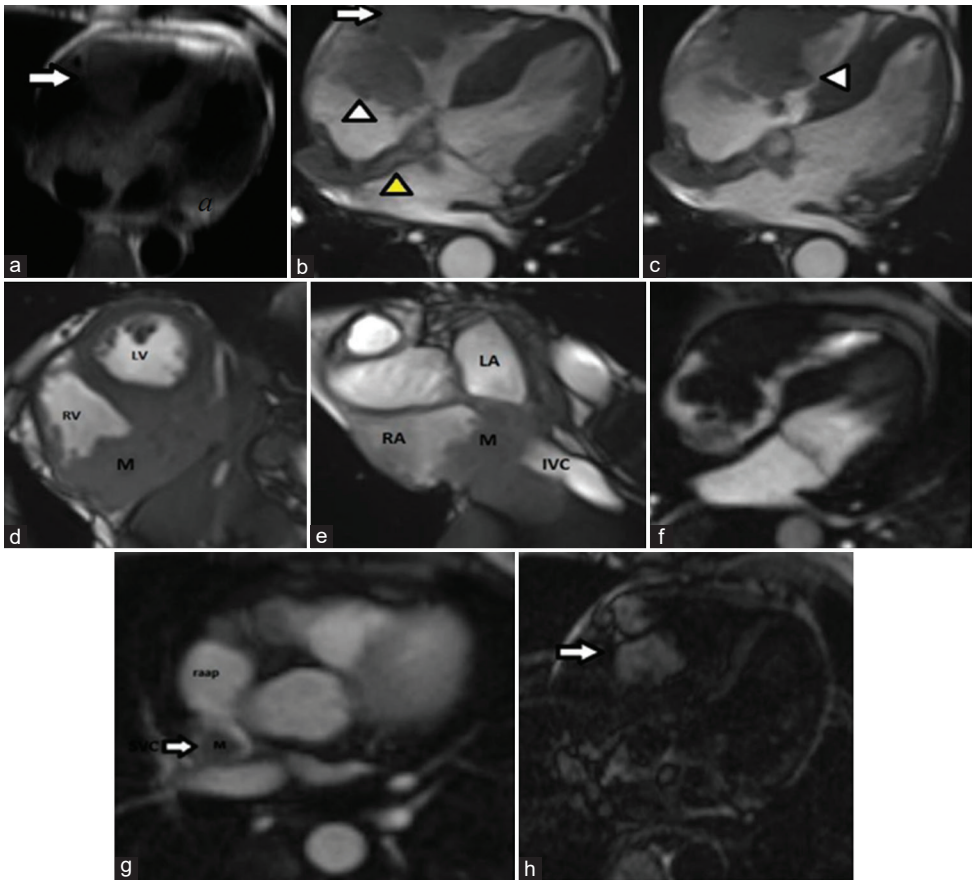

Figure 3: A 72 year old male with pancreatic cancer, complaining of dyspnea and cough of one month duration. Echocardiographic examination revealed right atrial soft tissue mass lesion for CMR assessment. (a) Black blood pool axial view image hardly assessed a right ventricular mass lesion exhibiting intermediate signal intensity (arrow). (b and c) White blood pool four chamber view images reveal a large right ventricular soft tissue mass lesion measuring 50x35 mm in size (arrow). This lesion is adherent and immobile. It is related to the anterior aspect of free right ventricular wall (below & adherent to tricuspid valve). This lesion is seen extending within right atrial chamber via a lobulated mobile soft tissue lesion (white arrow heads) measuring 33x26 mm in size (infiltrating anterior tricuspid leaflet) seen moving in and out within right atrium and right ventricular chambers. The inter-atrial septum also appears to be thickened and infiltrated (yellow arrow head). The mass lesion exhibits intermediate signal intensity in white blood pool images. (d and e) White blood pool short axis view images reveal that the soft tissue mass lesion (M) is infiltrating the pericardium and the diaphragm. The mass is also extending to the superior portion of the IVC. Dynamic images four chamber views. (f) The mass is more delineated in the dynamic images with no appreciable enhancement in early phase. (g) The mass lesion is seen extending to the SVC. (raa`p= Right atrial appendage, M= mass) (h) IR delayed post contrast four chamber view image show enhancement of the mass lesion (arrow).

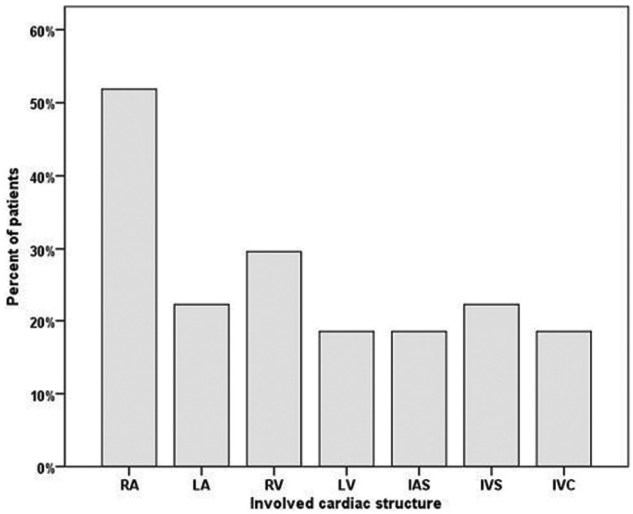

Chart 1: Bar chart showing the frequency of involvement of various cardiac structures in the study population.As regard the characteristics of the cardiac masses in our study, we found 40.7% (11/27) were mobile lesions while 59.3% (16/27) were immobile lesions, 92.6% (25/27) showed localized growth pattern while 7.4% (2/27) showed infiltrative diffuse pattern, 81.5% (22/27) showed regular outline and 18.5% (5/27) showed irregular outline.

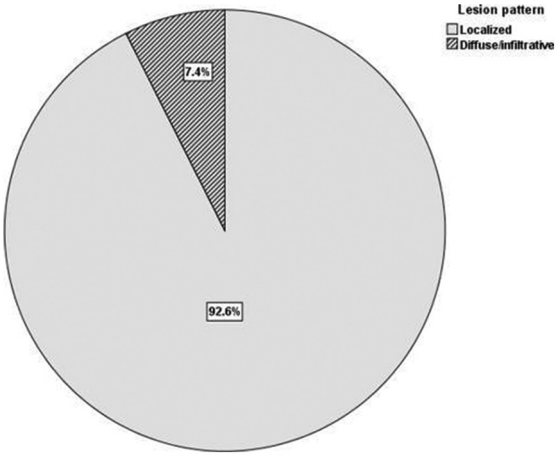

Chart 3: Pie chart showing the growth pattern of lesions in the study population.

Malik *et al.* [6] stated that the thrombus is the most common cause of a cardiac mass. Right atrial thrombi typically occur in patients with underlying coagulation disorders, atrial arrhythmias, central venous catheters, pacemaker leads, or a mechanical tricuspid valve. Braggion-Santos *et al*. [7] stated that a LV thrombus occurs in patients as sequel of myocardial infarction.

Most of the literatures such as Tao *et al*. [8] and Braggion-Santos *et al.* [7] described the thrombus to have variable MR-signal intensity, depending on the age of the thrombus. However, the most reliable MR feature is the absence of contrast uptake in the delayed contrast images as the thrombus is avascular. Rarely, large chronic thrombi may enhance peripherally due

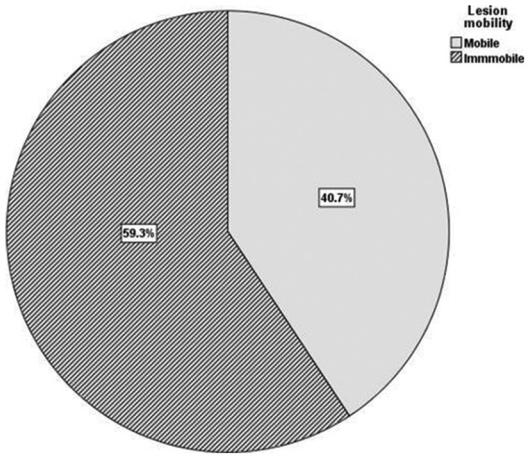

Chart 2: Showing the mobility of lesions in the study population.

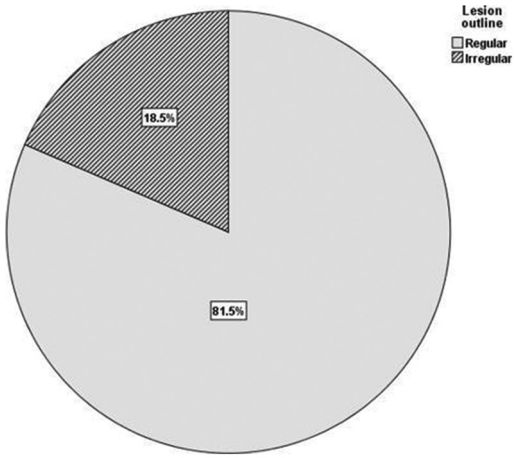

Chart 4: Pie chart showing the outline of lesions in the study population.

to neovascularization, and these cases can be diagnostically challenging.

So, our study and the previously mentioned studies and reviews agreed on the following items in the diagnosis of intracardiac thrombus: We also reported a case of focal hypertrophy of the septal wall that was misdiagnosed by echocardiography as a septal mass. On MRI, the focal hypertrophy followed the cardiac-wall SI in all sequences with no enhancement in delayed post-contrast images.

Kim *et al.* [9] stated that a mass-like hypertrophy of the left ventricular myocardium may mimic cardiac tumors. However, mass-like HOCM has more homogeneous signal characteristics and perfusion of the lesion is similar to the signal characteristics of the adjacent normal myocardium, except in the areas of fibrosis, whereas tumors often show varying degrees of signal heterogeneity before and after gadolinium administration. In addition, HOCM will show variable degrees of contractility, whereas a true mass will have no contractile portion [9].

We reported three cases of myxomas in our study, one of them was located at the left atrial, the other one was bi-atrial, and the

last one was a case of two myxomas located at the left atria and the left ventricle. All cases were mobile lesions with regular outline apart from one case that showed villous irregular surface. They exhibited variable SI in both black-blood-pool and white-blood-pool images, mostly intermediate-to-low SI compared with the myocardium with enhancement in the delayed post-contrast images.

Hoey *et al.* [10] mentioned that the majority cases of myxoma develop as a single lesion arises from the left atrium near fossa ovalis as pedunculated lesion with villous surface, while O'Donnell *et al.* [5] mentioned that the myxoma rarely arises in both atria and ventricles.

Beroukhim *et al.* [11] summarized in his study the main characteristics of myxoma, including irregular border, pedunculated, and mobile, hyperintense on T2-TSE, hypointense on early perfusion images, and heterogeneous enhancement on delayed-enhancement imaging, located in any cardiac chamber (commonly left or right atrium, or atrial septum) [11].

Our study and the previously mentioned studies and reviews agreed on the previous imaging of cardiac myxoma. We reported two cases of fibromas. Both were intramyocardial ventricular masses, one is located at the right ventricle and the other was located at the left ventricle. They showed regular outline and exhibited low signal intensity in both black-blood pool and white-blood-pool images. One of them shows intense enhancement in delayed post-contrast enhancement, while the other shows no enhancement.

Tao *et al.* [8] mentioned that fibroma is commonly located in the ventricular septum or ventricular free wall. It is a well-defined mass that exhibits hypo- to isointense on T1-weighted images and hypointense on T2-weighted images. Calcification is a relatively common feature.

Beroukhim *et al.* [11] summarized in his study the main characteristics of fibroma, including intramyocardial location along the ventricular septum or free wall, well-defined borders with a thin rim of myocardium, strong hyperenhancement on LGE imaging with or without a hypoenhancing (dark) core, hypointense on early perfusion images, and heterogeneous appearance on T1-weighted and T2-weighted FSE sequences, which agreed with our study results [11].

Three cases of rhabdomyomas were reported in our study. All of them were associated with tuberous sclerosis. One case showed a single cardiac mass, while the others were multiple masses.

Tao *et al.* [8] stated that rhabdomyomas can be multiple in more than 60% of cases. Multiplicity of rhabdomyomas has an even higher association with tuberous sclerosis. They are usually intramyocardial or intracavitary and located in the ventricles.

We reported four cases of malignant cardiac masses, two of them diagnosed as metastases, one was diagnosed as cardiac lymphoma, while the last one diagnosed as cardiac sarcoma.

All malignant cardiac masses showed irregular outline, 50% of them showed infiltrative pattern of growth, 50% of them showed pericardial infiltration and pericardial effusion. All of them showed variable degrees of enhancement in delayed postcontrast images.

Braggion-Santos *et al.* [7] also reported that most of the malignant lesions were generally large and heterogeneous with ill-defined margins, frequently occupying almost the entire affected chamber or multiple chambers of the heart. Pericardial or extracardiac structure invasion or valvular destruction may be identified.

We reported a case of lymphoma for a young adult patient with diffuse infiltrative lesion with irregular outline affecting both atria and IAS with encasement of the great vessels. They showed intermediate SI in both black-blood pool and white-blood-pool images with faint enhancement in delayed postcontrast images.

Kaminaga *et al.* [12] mentioned in his study that cardiac lymphoma showed isointense to slightly hyperintense to the myocardium on T1 SE and hyperintense on T2 SE, while Braggion-Santos *et al*. [7] reported in his study that cardiac lymphoma preferentially involves the right atrium, with invasion of adjacent structures and voluminous pericardial effusion.

As regards our study, the statistically significant items in the differentiation between the benign and the malignant lesions were the size of the lesion, the marginal outline, the pattern of growth, late gadolinium enhancement, and the pericardial affection, either pericardial infiltration or presence of pericardial effusion.

Benign lesions showed relatively small size, regular outline, and localized pattern of growth, with no pericardial infiltration, in comparison with the malignant lesions that show ill-defined irregular outlines with diffuse infiltrative pattern of growth, infiltration to the pericardium, as well as presence of pericardial effusion and extracardiac masses.

As regards the delayed enhancement in our study, all malignant lesions showed delayed enhancement compared with 69.6% of the benign lesions that showed no delayed enhancement.

The two cases that showed conflict in the diagnosis of their natures were myxoma versus thrombus and fibroelastoma versus thrombus, likely attributed to the small size of the lesions.

Follow-up studies were done to only seven cases out of the 13 cases that were diagnosed as pseudotumors and revealed that 57.1% (4/7) of the cases showed organization of the thrombus by TTE, 28.6% (2/7) showed complete resolution of the thrombus by CMRI and TTE.

In our study, the malignant lesions showed larger size with mean cross-sectional area 16.7 cm^2 in comparison with the benign lesions that showed mean cross-sectional area 4.4 cm^2 and that attends a statistically significant P value of 0.003 (significant $P < 0.05$).

All the benign lesions showed localized pattern of growth compared with 50% (2/4) of the malignant lesions that showed infiltrative pattern and 50% (2/4) showed localized pattern of growth with a statistically significant P value of 0.017 (significant $P < 0.05$).

As regards the marginal outline, 95.7% (22/23) of the benign lesions showed regular outline compared with the malignant lesions, which all of them showed irregular outline with a statistically significant difference.

All malignant lesions showed delayed enhancement compared with 69.6% of the benign lesions that showed no delayed enhancement with a statistically significant *P* value less than 0.021 (significant $P < 0.05$).

As regards the pericardial affection, none of the benign lesions showed pericardial infiltration compared with 50% (2/4) of the malignant lesions that showed pericardial infiltration with a statistically significant *P* value of 0.017.

Limitation

The relatively small number of the studied population with the need to involve larger number of patients in future studies for the validation of our findings.

Conclusion

To conclude, we suggest that CMR imaging has the potential to be the independent and stand-out imaging choice for assessment of cardiac masses. CMR provides the clinician the proper information needed for therapeutic planning without the need of invasive biopsy in most of the cases as CMR can efficiently differentiate between. Various types of benign tumors, between benign and malignant lesions, and between pseudotumors and true tumors, thus could easily draw the way for the clinician, either to follow up, go for therapeutic, or surgical management, that renders better diagnostic, and subsequently prognostic results.

Acknowledgements

The study was performed to evaluate the efficacy of MRI, in diagnosis, evaluation of cardiac masses, and characterization of cardiac masses, aiming at differentiation between neoplastic and nonneoplastic entities.

Financial support and sponsorship

Nil.

Conflicts of interest

There are no conflicts of interest.

References

1. Sparrow PJ, Kurian JB, Jones TR, Sivananthan MU. MR imaging of cardiac tumors. Radiographics 2005;25:1255-76.
2. Bruce C. Cardiac tumours: diagnosis and management. Heart 2011; 97:151–160.
3. Murugan M, Gulati G. MR and CT imaging spectrum of right-sided cardiac masses: apictorial essay. NJR 2012; 2:3.
4. Frank H. Evaluation of congenital heart disease and cardiac masses by magnetic resonance imaging. J Cardiol 2003; 10:19–25.
5. O'Donnell DH, Abbara S, Chaithiraphan V, Yared K, Killeen RP, Cury RC, *et al*. Cardiac tumors: Optimal cardiac MR sequences and spectrum of imaging appearances. AJR Am J Roentgenol 2009;193:377-87.
6. Malik SB, Kwan D, Shah AB, Hsu JY. The right atrium: Gateway to the heart—anatomic and pathologic imaging findings. Radiographics 2015;35:14-31.
7. Braggion-Santos MF, Koenigkam- Santos M, Teixeira SR. Magnetic resonance imaging evaluation of cardiac masses. Arq Bras Cardiol 2013; 101:3.
8. Tao TY, Yahyavi-Firouz-Abadi N, Singh GK, Bhalla S. Pediatric cardiac tumors: Clinical and imaging features. Radiographics 2014;34:1031-46.
9. Kim EY, Choe YH, Sung K, Park SW, Kim JH, Ko YH. Multidetector CT and MR imaging of cardiac tumors. Korean Journal of Radiology 2009;10:164-75.
10. Hoey ETD, Shahid M, Ganeshan A. MRI assessment of cardiac tumours: part 1, multiparametric imaging protocols and spectrum of appearances of histologically benign lesions. Quant Imaging Med Surg 2014; 4:478–488.
11. Beroukhim RS, Prakash A, Valsangiacomo Buechel ER, Cava JR, Dorfman AL, Festa P, *et al*. Characterization of cardiac tumors in children by cardiovascular magnetic resonance imaging: a multicenter experience. Journal of the American College of Cardiology 2011;58:1044-54.
12. Kaminaga T, Takeshita T, Kimura I. Role of magnetic resonance imaging for evaluation of tumors in the cardiac region. Radiology 2003; 13:L1–L10.